

Czochralski growth of Yb³⁺ and Pr³⁺ doped Ca-fluoroapatite

A. Caprez, P. Mikhail, C. Schwecke, and J. Hulliger

Department of Chemistry and Biochemistry, University of Berne, CH-3012 Berne, Switzerland

(Received 19 March 1997; accepted 12 August 1997)

Pure, Pr³⁺, and Yb³⁺ doped Ca-fluoroapatite (Ca-FAP) crystals were grown by the Czochralski method. The effective distribution coefficient k_{eff} for Yb³⁺ was 0.5. For Pr³⁺ a very high k_{eff} of 1.4 was obtained. Values for k_{eff} are discussed in terms of an elastic model accounting for the strain energy originating from the difference in the size of Ln³⁺ ions. The Ln³⁺ concentrations were measured by absorbance spectroscopy, by inductively coupled plasma optical emission spectroscopy, and by electron microprobe analyses.

The apatite structural family [A₁₀(MO₄)₆X₂], represented by a large class of natural and synthetic compounds, crystallizes in a few different, but related, hexagonal and pseudohexagonal structures.^{1,2} Ca₅(PO₄)₃F (Ca-FAP), apatite, belongs to the hexagonal space group *P*6₃/*m* with *Z* = 2.³ The ten Ca²⁺ ions are distributed over two crystallographically different sites: 4 Ca²⁺ are at site I with site symmetry 3 and 9-fold coordination by O²⁻; 6 Ca²⁺ are at site II with 6-fold O²⁻ and one F⁻ coordination.⁴ Lanthanide dopants predominantly enter the Ca(II) site which provides a low energy charge compensation mechanism⁵: The Ln³⁺ ion substitutes for Ca²⁺(II), whose nearest neighbor F⁻ ion is replaced by an O²⁻.⁶ Because only one F⁻ ion is available for bonding to every three Ca(II) ions, at most only two Ln³⁺ ions for every ten Ca²⁺ in the unit cell can enter the structure without creating an additional charge compensation mechanism.⁵ In this study we found that co-doping with, e.g., Na⁺ had no influence on the effective distribution coefficient k_{eff} of Yb³⁺.

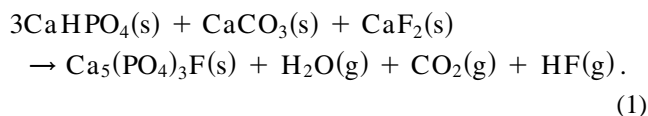
Yb³⁺ doped Ca-FAP and Sr-FAP are currently of interest because of efficient solid state laser properties when pumped by InGaAs diode sources.⁷⁻⁹ Recently, a diode-pumped, Q-switched Sr-FAP:Yb³⁺ laser (1047 nm) has been demonstrated.⁹

In this work we have explored Ca-FAP crystal growth for two reasons: (i) determination of the effective distribution coefficients k_{eff} of Yb³⁺ and Pr³⁺, and (ii) the potential of the Ca-FAP host-lattice as a new material for Pr³⁺ hyperfine pumped optical hole burning (H-OHB). An important parameter for the application of OHB in optical memories is the homogeneous linewidth of the holes, which is influenced by flip-flop processes of the nuclear magnetic moments of the host material.¹⁰ In a previous study we have discussed possible low nuclear spin density host materials for Pr³⁺ or Eu³⁺ H-OHB.¹⁰ However, a major drawback of selected compounds is that they showed only low doping levels and some effects of disorder in the nearest neighborhood of Ln³⁺ due to a heterovalent mechanism of substitution. Al-

though Ca-FAP will provide nuclear spins at P and F sites, it nevertheless bears the possibility of a particular mechanism for the charge compensation of Ln³⁺. The mechanism discussed above implies that a Pr³⁺ ion in the Ca-FAP lattice would be surrounded by 7 O²⁻ ions whose only isotope with nonvanishing spin (O¹⁷, *I* = 5/2, $\mu^{(N)} = -1.9 \mu_N$) has a very low natural abundance (0.04%).¹¹ In the first coordination sphere of the Pr³⁺ ion no nuclear magnetic moments could hence provide an efficient mechanism of broadening the homogeneous line.

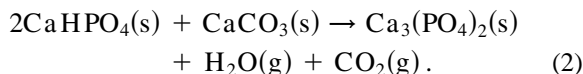
In the following we describe the Czochralski growth of Ca-FAP doped either by Yb³⁺ or Pr³⁺ and the determination of the effective distribution coefficients k_{eff} . Obtained values are discussed in terms of an elastic model accounting for the strain energy originating from the difference in the size of Ln³⁺ ions.

For Czochralski pulling we used the equipment as described recently.¹² Crystals were pulled from a 22 (Ø) × 25 mm Ir crucible under a constant Ar flow of 50 ml/min. CaCO₃ (Aldrich, purity: 99.95%), CaHPO₄ (Aldrich, purity: 99%), and CaF₂ (Aldrich, purity: 99.9%) were used as starting materials. In a first step stoichiometric amounts of the raw materials were shaken in a polyethylene bottle and sintered in a platinum crucible at 1100 °C for 60 h in a N₂ flow of about 100 ml/min. Crystals grown from a charge prepared in this way were opaque and consisted of at least two phases. A possible explanation is given by the Reaction (1):

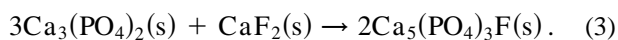


Formation of H₂O yielded a certain amount of hydroxyapatite in the starting powder, which led to inclusions during crystal growth. Precursor material was hence prepared in two steps: (i) water-free Ca₃(PO₄)₂ was obtained first according to Reaction (2) in air at a

temperature of 1000 °C (60–80 h).



In a second step (ii), $\text{Ca}_3(\text{PO}_4)_2$ obtained from Reaction (2) and CaF_2 were reacted. The latter was dried under a flow of 5% $\text{HF}/95\%$ N_2 gas (20–50 ml/min) at 1000 °C for 24 h. To prevent water contamination, the $\text{Ca}_3(\text{PO}_4)_2$ powder was taken from the furnace directly after finishing Reaction (2). Hot $\text{Ca}_3(\text{PO}_4)_2$ was mixed with the CaF_2 in a preheated mortar. After transferring into a hot Ir crucible, it was heated up in 2 h to 1700 °C in order to complete Reaction (3):



For Reactions (2) and (3) stoichiometric amounts of the starting materials were used. The melt (11–13 g) was superheated for 1 h 50 °C above the melting point. Spontaneous nucleation was initiated on a tapered Ir wire and crystals became single grain after ~2 mm of pulling. Spontaneous nucleation and seed selection produced crystals growing along the *c*-axis. For a pulling rate of 1.2 mm/h and a rotation of 45 rpm pale blue-greenish crystals of 30 mm in length and 10 mm in diameter were obtained. The boules showed opaque inclusions in the core extending along the *c*-axis. These defects may be caused by a lower curvature of the convex growth interface at larger diameters. The trapping of gas bubbles in the core of Ca-FAP crystals is a known imperfection.⁴ Slices with sufficient optical quality for spectroscopic measurements could be cut from the obtained crystals.

During growth experiments (24 h) vapor losses, which may lead to the described imperfections in the core of the crystal, were observed. Electron microprobe (EMP) and powder diffraction analysis of the losses, which were collected from the wall of the Czochralski apparatus, showed that substantial amounts of CaF_2 are lost during growth. In order to minimize these losses, an insulation lid (mullite) was placed at about 50 mm above the top of the crucible. Additionally, this particular insulation reduced the axial temperature gradient down to ~20–30 °C/cm. This was important to avoid cracking during the cooling process. A further precaution which proved to be a determinant in avoiding cracks was a slow cooling rate of 25 °C/h.

For doping experiments Pr_6O_{11} (Fluka, purity: 99.9%) or Yb_2O_3 (Fluka, purity: 99.9%) was added to the melt. Other growth parameters were the same as for pure Ca-FAP.

Small pieces of a crystal grown at a Pr^{3+} concentration in the melt of $c_0 = 0.07$ mol % (according to all atoms of Ca-FAP) were dissolved in HNO_3 (0.7 molar) and analyzed with the inductively coupled plasma optical

emission spectroscopy (ICP). The ICP technique led to $c_{\text{Pr}} = 0.1$ mol % in the crystal. Solutions of $\text{PrCl}_3 \cdot 6\text{H}_2\text{O}$ (Janssen Chemica, purity: 99.9%) in HNO_3 (0.7 molar) were used for calibration. An EMP analysis of a boule grown at $c_0 = 0.07$ mol % Pr^{3+} yielded a doping level of $c_{\text{Pr}} = 0.14$ mol %. In the case of the EMP measurement PrAlO_3 served as a reference for Pr^{3+} . The difference in the Pr^{3+} concentrations may originate from the reference material used in the EMP analysis. PrAlO_3 contains different elements when compared to Ca-FAP: Pr^{3+} and therefore, the software of the EMP calculated a different correction factor for the reabsorption of the characteristic x-ray of the Pr^{3+} . We assume that $k_{\text{eff}} = c_{\text{Pr}}/c_0 = 1.4$ obtained by the ICP method is more accurate.

The concentration for Yb^{3+} doping was determined spectroscopically. Based on the cross sections σ for the lines at 905 and 982 nm originating from the $^2\text{F}_{7/2} \rightarrow ^2\text{F}_{5/2}$ transition of Yb^{3+} and the measured absorbance at the maximums of these lines, the doping level was calculated. A sample grown at $c_0 = 0.28$ mol % Yb^{3+} and 0.5 mol % Na^+ in the melt was cut with flat and parallel faces perpendicular to the *c*-axis for absorption measurements with unpolarized light at room temperature (Fig. 1). With $\sigma_{905\text{nm}} = 2.6 \cdot 10^{-20}$ cm² and $\sigma_{982\text{nm}} = 5.3 \cdot 10^{-20}$ cm² for an electric field polarization perpendicular to the *c*-axis ($E \perp c$),¹³ we yielded $c_{\text{Yb}} = 0.13$ mol %, which corresponds to $k_{\text{eff}} = 0.5$.

Qualitatively, the influence of cations co-doping has been observed earlier.¹⁴ The value of k_{eff} for Yb^{3+} seems not to be significantly influenced by adding Na^+ to the melt. This is also consistent with the fact that we could not detect Na^+ by the proton induced gamma emission (PIGME)¹⁵ method in a crystal grown at melt concentrations $c_0 = 0.6$ mol % Na^+ and 0.3 mol % Yb^{3+} . The detection limit was 0.03 mol % Na^+ and a basalt (BHVO-1)¹⁶ served as Na reference.

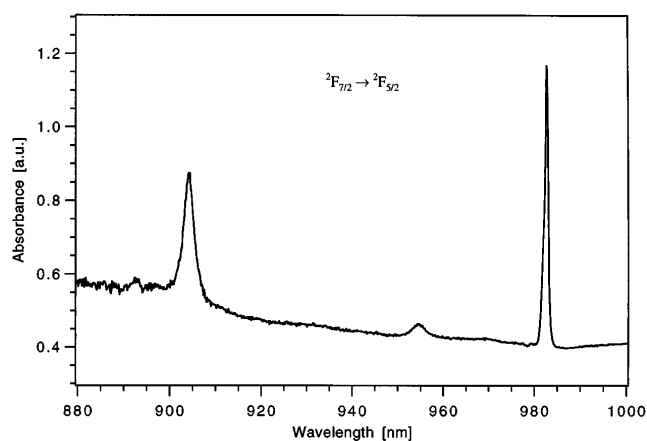


FIG. 1. Optical absorption spectrum of Yb^{3+} doped Ca-FAP ($c_{\text{Yb}} = 0.13$ mol %) at room temperature. The thickness of the sample was 3.24 mm and the spectrum was measured with unpolarized light propagating along the *c*-axis.

A possible explanation for a large difference in the k_{eff} for Yb^{3+} and Pr^{3+} could be due to the different ionic radii of the lanthanides. The electronic structures are very similar and the oxidation states are the same. The only variable affecting k_{eff} is most likely the ionic radii (0.98 Å for Yb^{3+} and 1.14 Å for Pr^{3+} , for a coordination number of 8).¹⁷ Brice¹⁸ regards the lattice as an elastic continuum and calculates the strain energy originating from the radius misfit between the substituted and the doping ion. The effective distribution coefficient k_{eff} depends on the misfit in the radius and on elastic properties:

$$\ln(k_{\text{eff}}) = \ln(k_0) - \frac{4\pi EN_A}{RT} \times \left[\frac{1}{2} r_A (r_j - r_A)^2 + \frac{1}{3} (r_j - r_A)^3 \right], \quad (4)$$

where k_0 is the effective distribution coefficient for a dopant with a radius misfit of zero, E is the averaged Young's modulus, N_A is the Avogadro number, T is the melting temperature of the material and r_A and r_j are the effective ionic radii of the substituted ion (index A) and the dopant (index j), respectively. Relation (4) was applied to estimate the ratio between the distribution coefficients of Yb^{3+} and Pr^{3+} ($k_{\text{eff}}^{\text{Yb}}/k_{\text{eff}}^{\text{Pr}} = 0.58$) using an effective ionic radius of 1.12 Å (for a coordination number of 8)¹⁷ for Ca^{2+} . Young's moduli for the direction parallel (E_{\parallel}) and perpendicular (E_{\perp}) to the 6-fold symmetry axis were calculated from the elastic constants of hydroxy-apatite.¹⁹ The average value $E = \frac{1}{3} \cdot (E_{\parallel} + 2 \cdot E_{\perp}) = 120$ GPa was used for Eq. (4). Payne *et al.*¹³ give an average value of $E = 119$ GPa for $\text{Ca}_5(\text{PO}_4)_3\text{F}$. The measured ratio of the two distribution coefficients is 0.36, being smaller than the calculated value (0.58). This may be caused by an uncertainty in the ionic radii, which after Brice¹⁸ can introduce an error of 20%. However, the model predicts a significantly larger k_{eff} for Pr^{3+} .

Optical absorption spectra for a Pr^{3+} doped crystal ($c_{\text{Pr}} = 0.1$ mol %) at room temperature to 11 K measured with unpolarized light propagating along the c -axis indicated that the linewidth of the ${}^3\text{H}_4 \rightarrow {}^1\text{D}_2$ transition exhibits only a low temperature dependence (Fig. 2). The half-width is decreasing only by a factor 1.4 (for the lowest crystal field level), which would mean that the broadening is mainly inhomogeneous. The room temperature absorption spectrum of an Yb^{3+} doped sample ($c_{\text{Yb}} = 0.13$ mol %) exhibits a half-width of 2.49 nm for the line at 905 nm ($E \perp c$) (Fig. 1). This is in agreement with the values of 2.4 nm (for $E \parallel c$) obtained earlier.^{20,21}

Preliminary experiments²² on $\text{Ca-FAP}:\text{Pr}^{3+}$ revealed no H-OHB processes. Maybe this is due to (i) the site symmetry m of the Pr^{3+} ion, which does not allow the transition in the lowest crystal field level,¹⁰ or (ii) the

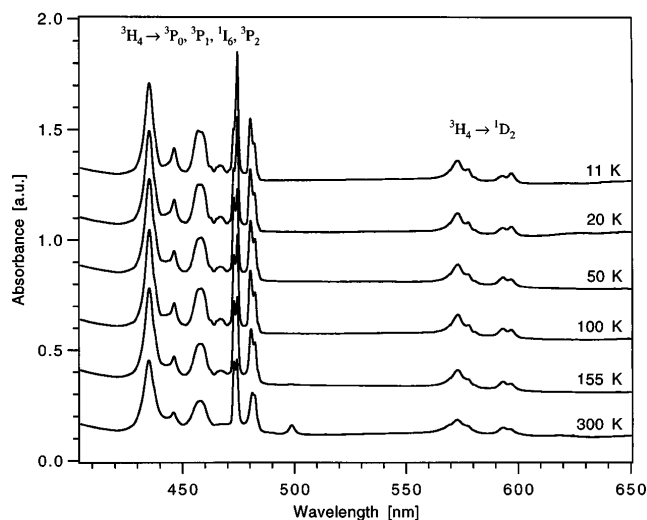


FIG. 2. Optical absorption spectra of Pr^{3+} doped Ca-FAP ($c_{\text{Pr}} = 0.1$ mol %) at 11 to 300 K. The thickness of the sample was 3.1 mm. All spectra were measured with unpolarized light propagating along the c -axis.

presence of a broad homogeneous line leading to an overlapping of the holes with the other hyperfine levels of the electronic ground state.

ACKNOWLEDGMENTS

We thank F. Graf and B. Plagemann of the group of Professor U. Wild at the ETH Zurich for helpful discussions and preliminary H-OHB experiments. We are indebted to Dr. L. Diamond for an introduction to electron microprobe analysis. We also thank Ch. Widmer and K. Noll of the group of Professor H. Gaggeler and Professor U. Krähenbühl (University of Berne) for providing an ICP analyzer and performing the PIGME experiments and the group of Professor H.U. Güdel (University of Berne) for using spectroscopic equipment. Both crystal growth and the electron microprobe at the Institute of Mineralogy and Petrography of the University of Berne were supported by the Swiss National Science Foundation (projects 2000-043116.95/1 and 21-26579.89, respectively). Further support was provided by the Wander Foundation (University of Berne).

REFERENCES

1. E. R. Kreidler and F. A. Hummel, *Am. Mineral.*, **55**, 170 (1970).
2. A. G. Cockbain, *Mineral. Mag.*, **36**, 654 (1968).
3. W. L. Bragg, *Atomic Structure of Minerals* (Cornell Univ. Press, Ithaca, NY, 1937).
4. G. B. Loutts and B. H. T. Chai, *SPIE-The International Society for Optical Engineering*, **1863**, 31 (1993).
5. L. D. DeLoach, S. A. Payne, W. L. Kway, J. B. Tassano, S. N. Dixit, and W. F. Krupke, *J. Lumin.*, **62**, 85 (1994).
6. J. L. Ouweltjes, *Modern Materials* (Academic Press, New York, 1965), Vol. 5, p. 161.

7. M. R. Dickinson, L. A. W. Gloster, N. W. Hopps, and T. A. King, *Opt. Commun.* **132**, 275 (1996).
8. C. D. Marshall, L. K. Smith, R. J. Beach, M. A. Emanuel, K. J. Schaffers, J. Skidmore, S. A. Payne, and B. H. T. Chai, *IEEE J. Quantum Electron.* **32**, 650 (1996).
9. L. A. W. Gloster, P. Cormont, A. M. Cox, T. A. King, and B. H. T. Chai, unpublished.
10. A. Caprez, P. Meyer, P. Mikhail, and J. Hulliger, *Mater. Res. Bull.* **32**, 1045 (1997).
11. *Handbook of Chemistry and Physics*, 74th ed., edited by D. R. Lide and H. P. R. Frederikse (CRC Press, Cleveland, OH, 1993–94), Sec. 11, p. 35.
12. A. Caprez, P. Mikhail, and J. Hulliger, *J. Cryst. Growth* (1997, in press).
13. S. A. Payne, L. K. Smith, L. D. DeLoach, W. L. Kway, J. B. Tassano, and W. F. Krupke, *IEEE J. Quantum Electron.* **30**, 170 (1994).
14. R. C. Ohlmann, K. B. Steinbruegge, and R. Mazelsky, *Appl. Opt.* **7**, 905 (1968).
15. J. R. Bird and E. Clayton, *Nucl. Instrum. Methods Phys. Res.* **218**, 525 (1983).
16. F. J. Flanagan, Geological Survey Professional Paper 840, United States Government Printing Office, Washington (1976).
17. R. D. Shannon and C. T. Prewitt, *Acta Crystallogr.* **B25**, 925 (1969).
18. J. C. Brice, *J. Cryst. Growth* **28**, 249 (1975).
19. *Handbook of Physical Constants*, edited by S. P. Clark, Jr. (The Geological Society of America, Inc., New York, 1966), p. 142.
20. S. A. Payne, L. D. DeLoach, L. K. Smith, W. L. Kway, J. B. Tassano, W. F. Krupke, B. H. T. Chai, and G. Loutts, *J. Appl. Phys.* **76**, 497 (1994).
21. L. D. DeLoach, S. A. Payne, L. K. Smith, W. L. Kway, and W. F. Krupke, *J. Opt. Soc. Am. B* **11**, 269 (1994).
22. Measurements at ETH Zurich, Laboratory of Physical Chemistry.